

Article

Towards Solving the “*Colomerus vitis* Conundrum”: Genetic Evidence Reveals a Complex of Highly Diverged Groups with Little Morphological Differentiation

Davina L. Saccaggi ^{1,2,*}, Palesa Maboei ³, Chanté Powell ³, Nompumelelo P. Ngubane-Ndhlovu ¹, Elleunorah Allsopp ⁴, James Wesley-Smith ⁵ and Barbara van Asch ^{3,*}

- ¹ Plant Health Diagnostic Services, Department of Agriculture, Land Reform and Rural Development, Private Bag X5015, Stellenbosch 7599, South Africa; nompumelelond@dalrrd.gov.za
- ² Citrus Research International, P.O. Box 2201, Matieland 7602, South Africa
- ³ Department of Genetics, University of Stellenbosch, Private Bag X1, Matieland 7602, South Africa; pmaboei@gmail.com (P.M.); chantepowell4@gmail.com (C.P.)
- ⁴ Agricultural Research Council, Infruitec-Nietvoorbij, Private Bag X5026, Stellenbosch 7599, South Africa; allsoppe@arc.agric.za
- ⁵ Electron Microscope Unit, Sefako Makgatho Health Sciences University, Molotlegi Street, Ga-Rankuwa Zone 1, Ga-Rankuwa 0208, South Africa; jaimewesley-smith@smu.ac.za
- * Correspondence: davinas@cri.co.za (D.L.S.); bva@sun.ac.za (B.v.A.)



Citation: Saccaggi, D.L.; Maboei, P.; Powell, C.; Ngubane-Ndhlovu, N.P.; Allsopp, E.; Wesley-Smith, J.; van Asch, B. Towards Solving the “*Colomerus vitis* Conundrum”: Genetic Evidence Reveals a Complex of Highly Diverged Groups with Little Morphological Differentiation. *Diversity* **2022**, *14*, 342. <https://doi.org/10.3390/d14050342>

Academic Editors: Michael Wink and Agnieszka Napierała

Received: 24 March 2022

Accepted: 19 April 2022

Published: 28 April 2022

Publisher’s Note: MDPI stays neutral with regard to jurisdictional claims in published maps and institutional affiliations.



Copyright: © 2022 by the authors. Licensee MDPI, Basel, Switzerland. This article is an open access article distributed under the terms and conditions of the Creative Commons Attribution (CC BY) license (<https://creativecommons.org/licenses/by/4.0/>).

Abstract: *Colomerus vitis* is a pest of grapevine worldwide that includes three strains recognised by plant symptoms (bud, erineum, and leaf curl), which could represent cryptic species. We approached this long-standing question by integrating genetic and morphological methods. COI sequences of mites from South Africa and other countries showed five phylogenetic groups (G1 to G5) with intergroup *p*-distances up to 23% and intragroup divergence lower than 2%. The three groups found in South Africa (G1, G2, and G3) were screened from a variety of grapevine samples using a novel multiplex PCR method. Only G1 and G3 were significantly associated with erineum and buds, respectively, and the three groups were frequently co-present in the same plant sample. Cryo-SEM showed adults with five- and six-rayed empodia, variable microtubercle shape, and prodorsal shield patterns. Specimens with six-rayed empodia and a smooth prodorsal shield were more often associated with buds, while specimens from erineum were variable. These results support the genetic evidence in that particular groups or morphotypes are not associated exclusively with specific plant niches. We propose that *C. vitis* is a complex of at least five genetically distinct but morphologically similar species, and that no one species can be assigned to a particular grapevine symptom.

Keywords: cryo-SEM; Eriophyidae; genetic divergence; grapevine; phylogenetics

1. Introduction

Colomerus vitis (Pagenstecher) (Trombidiformes: Eriophyidae) is found on the cultivated grapevine, *Vitis vinifera* L., worldwide [1]. *Colomerus vitis* is generally hypothesised to comprise three strains recognised by the three symptoms exhibited by the host plant, namely, bud, erineum, and leaf curl [2]. No morphological differences between the strains have been identified; therefore, according to traditional taxonomy, they are considered conspecific [3]. However, there has long been debate as to whether the three strains may represent three symptom-specific species, especially since Smith and Stafford [2] asserted that each strain is only able to produce that particular symptom.

The current taxonomic literature recognises two species of *Colomerus* on grapevine, namely, *C. vitis* and *C. oculivitis* (Attiah) [4–7]. *Colomerus vitis* descriptions vary in the depiction and description of microtubercle shape, prodorsal shield pattern, and ridges on the female genital coverflap, while they remain consistent in recording the number of empodial rays as five [3–6,8]. Although a number of characteristics have been described

as different between *C. vitis* and *C. oculivitis*, the only unambiguous one is the five-rayed empodia in *C. vitis*, while *C. oculivitis* has six-rayed empodia [4,6,7]. Given the multiple strains of *C. vitis* and the overlap in descriptions of *C. vitis* and *C. oculivitis*, Craemer and Saccaggi [4] hypothesised that *C. oculivitis* may represent the bud form of *C. vitis*. Differentiation of *C. vitis* strains has been unsuccessful to date, due partially to their small size and lack of phylogenetically informative features.

The debate as to the species status of *C. vitis* has intensified in recent years, as genetic studies have provided varying results. Carew et al. [9] found sufficient genetic variation in the internal transcribed spacer I (ITS-1) region and microsatellites to consider the bud and erineum strains of *C. vitis* to be separate species. In contrast, Valenzano et al. [10] found no differences in the ITS-1 sequences of *C. vitis* collected from buds and erinea from a single vineyard in Apulia, Italy.

Delineation of species is challenging when the organisms in question are small, have similar morphology, and are characteristic-poor [11–14]. Such is the case within the superfamily Eriophyoidea, where species complexes often exist without clear morphological differentiation [12,15–22]. Differentiation of such species benefits greatly from employing an integrative taxonomic approach, where multiple taxonomic tools can be independently and jointly applied to species delineation. This approach has been successfully applied in a number of eriophyid species complexes to elucidate species status and relationships [14,18,21–25].

In this study, we adopted an integrative approach to investigate the genetic and morphological variation present in putative *C. vitis* mites. The genetic approach included DNA barcoding and phylogenetic clustering, as well as a novel multiplex PCR for the survey of a large number of samples. Morphologically, we examined individually collected mites using cryo-SEM imaging to show features on the mites' tiny bodies. Integrating these methods greatly enhanced our understanding of the diversity present in *C. vitis*.

2. Materials and Methods

2.1. Grapevine Mite Samples

Samples of grapevine eriophyid mites or DNA sequences came from multiple main sources (Table S1): (1) eriophyoids on imported grapevine material from various countries, detected and collected upon interception in South Africa by the laboratories of the Department of Agriculture, Land Reform, and Rural Development (DALRRD) [26]; (2) eriophyoids collected from vineyards in South Africa by Dr. Charnie Craemer (Agricultural Research Council) or by co-authors C.P. and P.M. during this study; (3) COI sequences of *C. vitis* deposited in Genbank (accession numbers MN164416 to MN164427; unpublished). In field collections, symptomatic plant tissues were collected and stored in separate sealed bags to avoid cross-contamination and kept cool until examination using a stereomicroscope. Samples were then prepared specifically for genetic and morphological analyses.

Mites for genetic analyses were collected either individually or by excising the infested plant tissue using sterile implements and transferred to a microtube containing 100 μ L of absolute ethanol. Individually collected mites were used for Sanger sequencing, while excised plant tissue was used for multiplex PCR analyses. Manual collection of mites allows for greater assurance of the presence and number of mites in the sample but is extremely time-consuming and requires skilled labour. Therefore, samples for multiplex PCR analyses were prepared by vigorous shaking of the microtube to dislodge the mites, followed by filtration by centrifugation through a 0.95 mm steel mesh that retained most of the plant material. The filtered ethanol containing the mites was evaporated on a heat block at 45 °C until the pellet was dry for subsequent DNA extraction. This "brute force" method allowed for screening of a large number of samples, but the number of mites isolated from the plant sample in this way was not quantified. For cryo-SEM, mites were kept alive on freshly collected plant tissue until processing.

2.2. Genetic Analyses

2.2.1. DNA Extraction, PCR Amplification, and DNA Sequencing

DNA was extracted using the Qiagen QIAamp DNA Micro Kit (QIAGEN) following the Isolation of Genomic DNA from Tissues protocol, with half volumes of all reagents. The standard COI barcoding region was amplified using the universal primer pair LCO1490 and HC02198 [27]. PCR amplifications were conducted in total volumes of 5 μ L, comprising 1 \times QIAGEN Multiplex PCR kit (QIAGEN), 10 ng/ μ L of DNA template, and 0.5 μ M of each primer. Thermocycling conditions consisted of 95 $^{\circ}$ C for 15 min, then 35 cycles of 94 $^{\circ}$ C for 30 s, 54 $^{\circ}$ C for 90 s, and 72 $^{\circ}$ C for 90 s, followed by 72 $^{\circ}$ C for 10 min. PCR products were Sanger-sequenced in the forward direction or bidirectionally (when the forward direction resulted in poor-quality sequences) with the BigDye Terminator v3.1 Cycle Sequencing Kit (Applied Biosystems) at the Central Analytical Facilities of the University of Stellenbosch, South Africa. All COI sequences were manually inspected and curated for ambiguities, and low-quality sequences were excluded from the dataset. All sequences were translated for the detection of potential premature stop codons and indels indicative of spurious amplification of nontarget DNA in Geneious Prime 2022.0.2 [28,29] (accessed in December 2021), using the invertebrate mitochondrial genetic code. The sequences generated in this study ($n = 31$) were deposited on GenBank under the accession numbers ON060625-ON060655.

2.2.2. Multiplex PCR

The initial Sanger sequencing of COI using universal barcoding primers showed superimposed peaks at some nucleotide positions indicating that pooled mites from the same sample contained mixtures of different genetic groups. Nevertheless, it was possible to clearly distinguish three genetic groups that were designated G1, G2, and G3. This fact, coupled with the need to screen a large number of samples, led to the design of a multiplex PCR based on three primer pairs specific to each of the three genetic groups (Table 1). The group-specific primers were designed to amplify fragments between 162 and 433 bp, with at least a 100 bp difference in amplicon size (Figure 1).

Table 1. List of primers used for singleplex PCR, Sanger sequencing, and multiplex PCR of the COI region in eriophyoid grapevine mites. Amplicon size includes the primers.

Primer Name	Sequence (5'–3')	Amplicon (bp)	Primer Type	Reference
LCO1490 HC02198	GGTCAACAAATCATAAAGATATTGG TAAACTTCAGGGTGACCAAAAATCA	710	Universal	Folmer et al. [27]
G1-F G1-R	GAATAGAATTATCGCAGACAGG CTAACACGATCTATACAAGAC	433	Group-specific	This study
G2-F G2-R	GCGTCTAGAACTATCTCAAAC TCATTACAACCAAGCATCAATG	162	Group-specific	This study
G3-F G3-R	ACGAATGGAATTGTCTCATAC CCAGAAGCTAACAAAGAGGA	252	Group-specific	This study

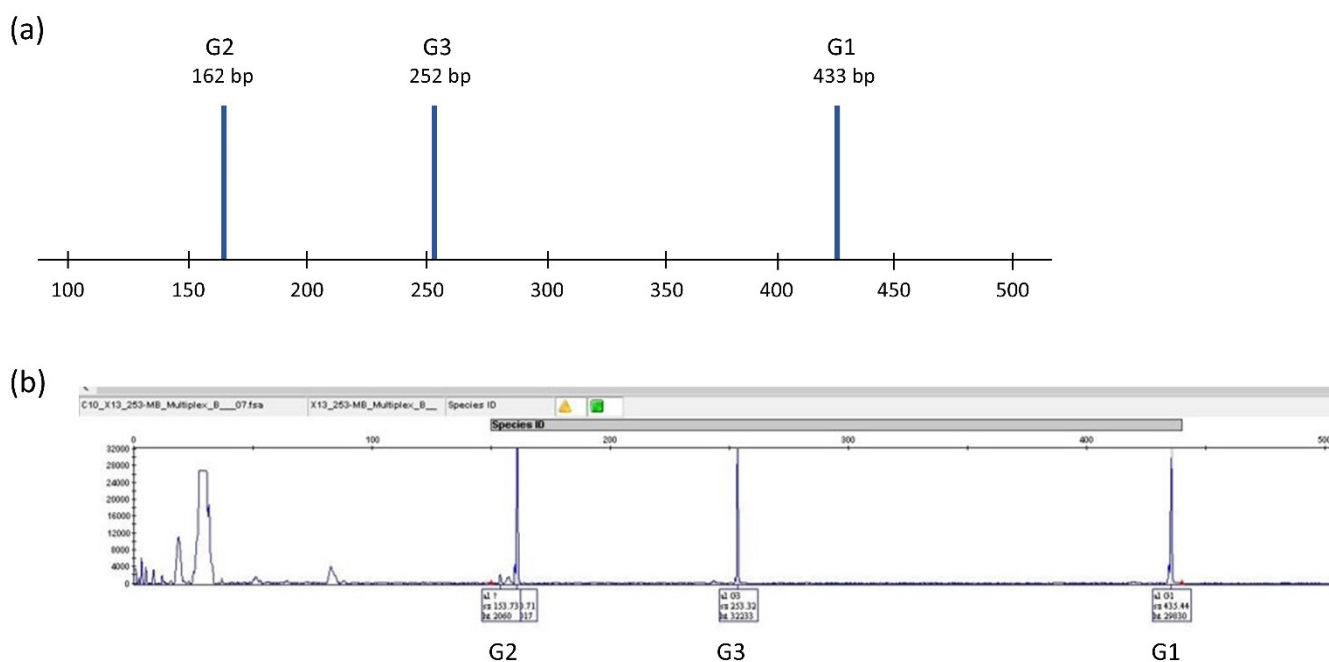


Figure 1. (a) Graphic representation of group-specific amplicons for multiplex PCR amplification of eriophyoid grapevine mites and fragment size detection by capillary electrophoresis. (b) Example of electropherogram of sample with co-presence of the genetic groups G1, G2, and G3.

All primers were tested for specificity in singleplex and multiplex reactions using DNA extracts previously identified by Sanger sequencing as belonging to one of the genetic groups, under the PCR and sequencing conditions described above. Group-specific PCR amplicons were further Sanger-sequenced for validation of the expected PCR product. Multiplex PCR amplifications were performed using 6-FAM-labelled forward primers in a total volume of 5 μ L comprising 1 \times QIAGEN Multiplex PCR kit, 0.5 μ M of each primer, and \sim 10 ng/ μ L DNA template. Thermocycling conditions were as follows: 95 $^{\circ}$ C for 15 min; 27 cycles at 94 $^{\circ}$ C for 30 s, 54 $^{\circ}$ C for 90 s, 72 $^{\circ}$ C for 90 s; 72 $^{\circ}$ C for 10 min. Capillary electrophoresis for fragment size detection was performed with LIZ600 as an internal size standard at the Central Analytical Facilities of Stellenbosch University. The data were analysed using GeneMapper Software Version 4.0 (Applied Biosystems), with bins defined for the expected fragment size of each genetic group. The multiplex PCR was used to screen 274 samples collected from five farms in the Western Cape and one in the Northern Cape Provinces of South Africa (Table S1) for the presence of G1, G2, and G3, the genetic groups previously detected in local vineyards by Sanger sequencing.

2.2.3. Phylogenetic Analysis and Genetic Divergence

Phylogenetic analysis for identification of genetic groups was based on the COI sequences generated in this study and sequences available on GenBank (accessed in November 2021) (Table S1), with *Eriophyes padi* Domes (GenBank KT070227) as the outgroup. Multiple sequence alignments were performed with MAFFT v7.450 [30] in Geneious Prime. The final alignment was 584 bp long. A maximum likelihood (ML) tree was constructed in IQ-TREE [31]. The best partitioning scheme was based on the edge-linked greedy strategy [32] using automatic model selection [33,34]. Nodal support was based on ultrafast bootstrap [35,36]. The final tree was drawn using FigTree v1.4.4 (<http://tree.bio.ed.ac.uk/>, accessed on 21 December 2021). Genetic divergence within and between the phylogenetic clusters identified in the ML tree was estimated as intragroup maximum pairwise distance (p -distance) and intergroup average p -distances calculated in MEGAX [37] using the Kimura two-parameter (K2P) model [38] with pairwise deletion of sites and bootstrap support test of 1000 replicates.

2.3. Morphological Analyses

A cryo-fixation technique adapted from Rahbani et al. [39] was used to prepare the mites for imaging. Mites were collected from plant tissue using a stereomicroscope and transferred to double-sided carbon tape on a specimen carrier. This was frozen by rapidly plunging it into subcooled liquid nitrogen ($-210\text{ }^{\circ}\text{C}$) for a few milliseconds to avoid ice crystal formation, transferred under vacuum and without warming to the precooled stage of the cryo-preparation chamber ($-140\text{ }^{\circ}\text{C}$), heated to $-100\text{ }^{\circ}\text{C}$ for 3 to 5 min to sublimate any water condensed on the surface of the mites, and then cooled again to $-140\text{ }^{\circ}\text{C}$ before sputter-coating with platinum for 60 s. Mites were imaged using a Zeiss Supra 55VP SEM equipped with a Gatan Alto cryo-stage (Gatan, Pleasanton, CA, USA). As SEM is limited by the orientation of the specimen on the stub, it was not possible to observe all the characteristics on each specimen. Images were focused on the characteristics recommended by Amrine and Manson [40] and de Lillo et al. [41] as essential for eriophyoid species descriptions. Images of the whole body, prodorsal shield, coxal area, and genitalia and legs were captured, wherever possible. Additionally, images of the empodia of the legs and the shape of the surface microtubercles were also captured, as these characteristics are important in the identification of the *Colomerus* species described on grapevine [4,6].

3. Results

3.1. Genetic Analyses

Sanger sequencing using universal primers resulted in a number of ambiguous nucleotides caused by superimposed peaks indicating the presence of multiple genetic groups in the same sample. Consequently, group-specific primers were designed on the basis of the initial sequences obtained with universal primers and optimised to amplify each of the genetic groups separately for subsequent Sanger sequencing, and for screening of a large number of samples by multiplex PCR.

3.1.1. Phylogenetics and Genetic Clustering

The phylogenetic tree included the novel COI sequences generated in this study ($n = 31$), as well as 11 sequences of *C. vitis* from Iran available on GenBank (Figure 2). Five phylogenetic clusters (G1 to G5) were recovered, with nodal support varying between 68% and 100%. Three of the clusters comprised sequences from a single country: G2 ($n = 5$) from South Africa, G4 ($n = 2$) from the USA, and G5 ($n = 7$) from Iran. G1 included sequences from South Africa ($n = 6$) and Iran ($n = 4$), while G3 was the most geographically diverse group with sequences from South Africa ($n = 13$), Spain ($n = 2$), the USA, Egypt, and Israel (each $n = 1$) (Figure 3). It is worth mentioning that 12 sequences from Iran were available on GenBank, but one (MN164425) was excluded from the phylogenetic tree because it produced a highly diverged branch that suggested the presence of artefactual polymorphisms.

Overall, the max p -distance was 24.76%, indicating the presence of non-conspecific sequences in the total dataset. The max p -distance within each phylogenetic cluster ranged between 0.00% (G1, G2, and G4) and 1.57% (G3), indicating that the sequences in each of the five phylogenetic clusters are conspecific (Tables 2 and 3). Average p -distances between groups ranged between 17.78% for the pair G3/G4 and 23.72% for the pair G2/G3, indicating that each phylogenetic cluster is a diverged genetic group. This pattern of high intergroup divergence and low intragroup divergence supports the hypothesis that the genetic groups/phylogenetic clusters likely represent separate species.

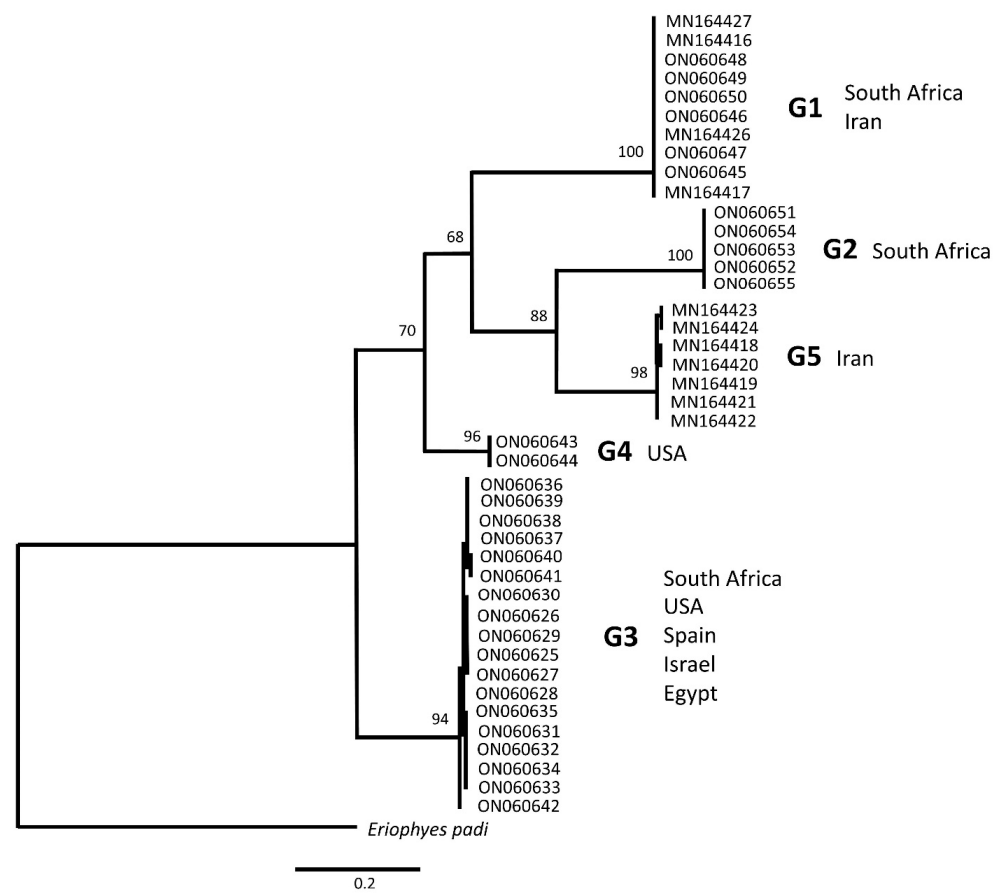


Figure 2. Maximum likelihood tree of COI sequences ($n = 42$; 584 bp) showing five genetic clusters of eriophyoid grapevine mites "*Colomerus vitis*" and their geographic distribution. Nodal support was based on 1000 bootstrap replicates.

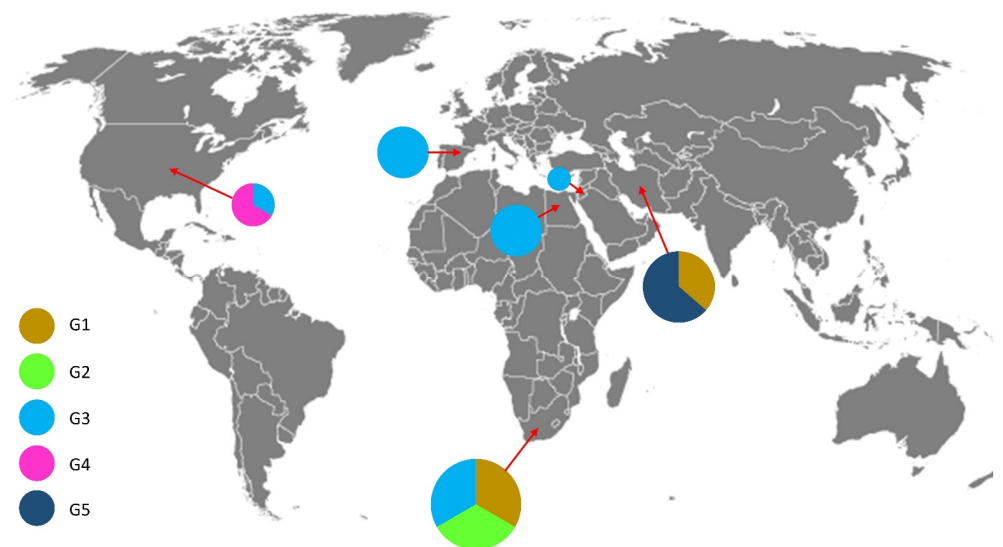


Figure 3. Geographic distribution of five genetic groups of eriophyoid grapevine mites, as determined by COI sequence variation.

Table 2. Maximum intragroup *p*-distances among five genetic groups (G1 to G5) of eriophyoid grapevine mites based on COI barcoding sequences (584 bp).

Genetic Group	Sample Size (<i>n</i>)	Max <i>p</i> -Distance (%)
Group 1	10	0.00
Group 2	5	0.00
Group 3	2	1.57
Group 4	18	0.00
Group 5	7	0.86
All sequences	42	24.76

Table 3. Average intergroup *p*-distances (%) among five genetic groups (G1 to G5) of eriophyoid grapevine mites based on COI barcoding sequences (584 bp). Standard errors are shown above the diagonal.

	Group 1	Group 3	Group 4	Group 2	Group 5
Group 1		2.30	1.90	2.28	2.04
Group 3	23.13		1.92	2.40	2.12
Group 4	18.33	17.78		2.26	2.01
Group 2	23.56	23.72	22.04		2.13
Group 5	20.01	20.72	19.41	19.59	

3.1.2. Association of Genetic Groups with Plant Symptoms

A total of 274 grapevine samples infested with eriophyoid mites were screened by multiplex PCR for the presence of the three genetic groups (G1, G2, and G3) identified from *Colomerus* mites by Sanger sequencing in samples collected in South Africa (Table S1). Each sample was collected from a single plant tissue type, namely, buds, erineae, or leaf curl symptoms. Overall, 195 of these samples (117 from buds, 73 from erineae, and five from leaf curl) were positive for the presence of mites of G1, G2, or G3, either exclusively or in mixtures (Figure 4). A total of 79 samples (28.8%) failed to yield amplicons, most likely due to insufficient number of mites recovered from the plant tissue during the centrifuging extraction method.

Overall, G2 was the most commonly detected group by multiplex PCR, as it was present in 62.6% of all samples analysed (49.5% of buds, 82.2% of erineae, and 80% of leaf curl) (Figure 5). G3 was detected in 55.9% of all samples (78.6% of bud samples, 23.3% of erineae samples, and none in leaf curl samples), and G1 was the least frequent group (37.4% overall, 15.4% of bud samples, 72.6% of erineae samples, and 40% of leaf curl samples). Specific groups were significantly associated with specific plant niches. G1 was significantly associated with erineae ($\chi^2 = 38.9$, $df = 2$, $p = 4.1 \times 10^{-9}$), and G3 was significantly associated with buds ($\chi^2 = 96.0$, $df = 2$, $p = 1.4 \times 10^{-21}$), while G2 showed no significant association with plant niche.

More than one genetic group was commonly detected in the same sample, with 48.2% of samples displaying genetic mixtures. This differed significantly between the different plant niches, with erineae more likely to have multiple genetic groups present (genetic mixtures in 64.4% of erineae samples) compared to buds and leaf curl (genetic mixtures in 39.3% and 20% of samples, respectively) ($\chi^2 = 40.9$, $df = 2$, $p = 1.3 \times 10^{-9}$). Since not all types of plant niches could be sampled at each collection site, it was further investigated whether the different distribution patterns of the genetic groups could be influenced by collection site (Figure 5). Again, mixtures of groups were common at all collection sites, but only the presence or absence of specific groups was compared, regardless of whether they were detected exclusively or in conjunction with other groups. Overall, there were significant differences in the distribution of genetic groups detected from different collection sites. These differences were more pronounced between sites from different geographic regions

within South Africa but were still significant between sites from the same region. Since this could be due to different plant niches sampled at different collection sites, samples from buds and erineae were compared between different collection sites (leaf curl was excluded due to small sample size). Significant differences in genetic groups present persisted, even when only comparing a specific sample type (buds (G1/G2/G3): $\chi^2 = 95.5/141.2/43.4$, $df = 5$, $p < 0.0001$; erineae (G1/G3): $\chi^2 = 80.5/209$, $df = 3$, $p < 0.0001$). Within sites from which more than one plant niche was collected, significant differences in the distribution of genetic groups in mites from buds and erineae remained (again, leaf curl was excluded due to small sample sizes). G3 was significantly associated with buds at three of the four collection sites analysed (sites 6/7/8: $\chi^2 = 33.3/20.3/43.2$, $df = 1$, $p < 0.0001$), G1 was significantly associated with erineae at site 7 ($\chi^2 = 52.4$, $df = 1$, $p = 4.6 \times 10^{-13}$), and G2 was significantly associated with erineae at site 5 ($\chi^2 = 68.1$, $df = 1$, $p = 1.6 \times 10^{-16}$).

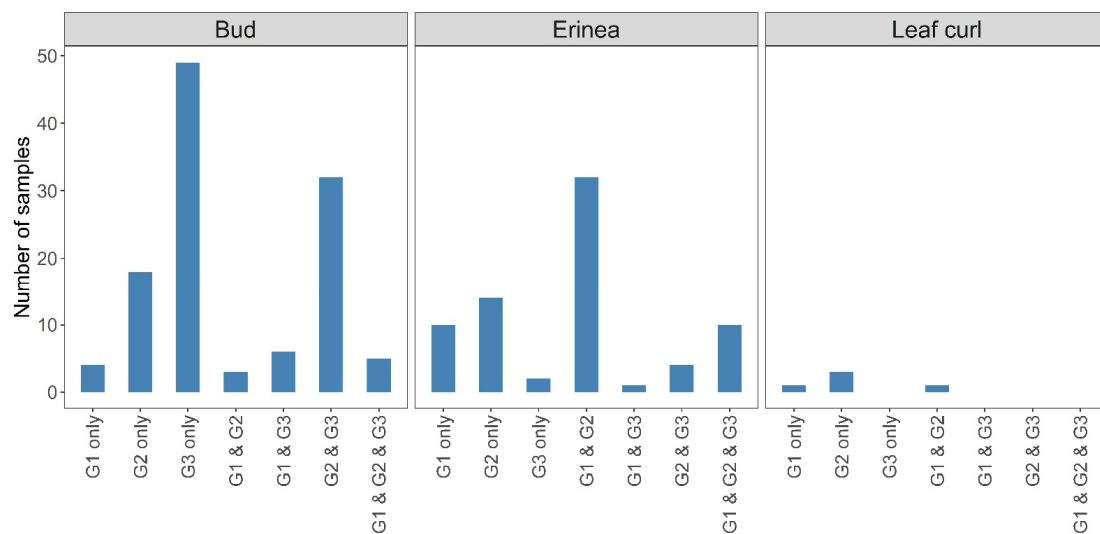


Figure 4. Genetic groups (G1, G2, and G3) and their mixtures detected in samples screened by multiplex PCR. Results from all sample sites are pooled.

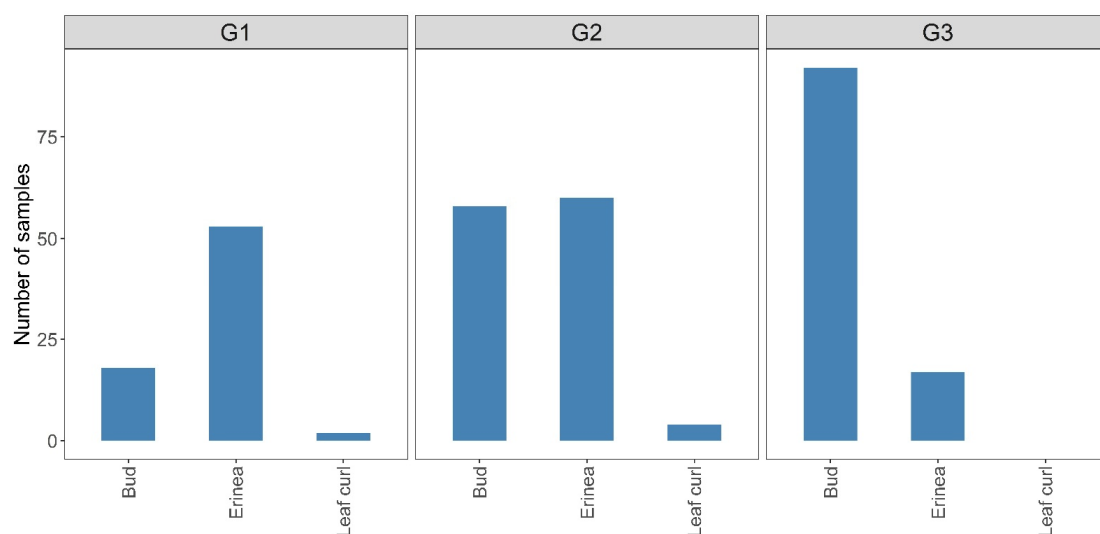


Figure 5. Presence of the three genetic groups detected in South Africa (G1, G2, and G3), regardless of whether they were detected alone or in a mixture with other groups, arranged by plant niche from which they were collected.

3.2. Morphological Analyses

Seventy mite specimens from site 7 were examined using cryo-SEM, 48 of which were collected from leaf erineae (28 females, one male, 16 adults of unknown sex, and three immatures) and 22 from buds (12 females, one male, and nine adults of unknown sex) (Table S1). Differences in characteristics could be observed between specimens (Table S2); however, because visible characteristics were limited by the orientation of the specimen, we could not always determine the sex of the specimen nor compare the full suite of characteristics across the whole dataset.

3.2.1. Whole Body

As is consistent with the description of this genus, all specimens observed were vermiform, with little dorsoventral differentiation.

3.2.2. Prodorsal Shield

Thirty specimens (21 from erineae and nine from buds) were orientated correctly to allow imaging of the prodorsal shield (Figure 6). The prodorsal shield pattern varied from having distinct ridges with at least the median and admedian lines complete, through various degrees of broken ridges to entirely smooth on the dorsal surface. The lateral surface to either side of setae was always patterned with ridges forming a distinct eye-like shape. Part of the prodorsal shield was observed in an immature specimen, which was pebbled with no clear ridges or eye-like shape visible. Shield pattern was significantly associated with the plant niche from which the mites were collected ($\chi^2 = 119.9$, $df = 1$, $p = 6.8 \times 10^{-28}$), with smooth or partially smooth prodorsal shields associated with buds (100% of bud specimens observed) and strongly patterned prodorsal shields associated with erineae (80% of erineae specimens observed).

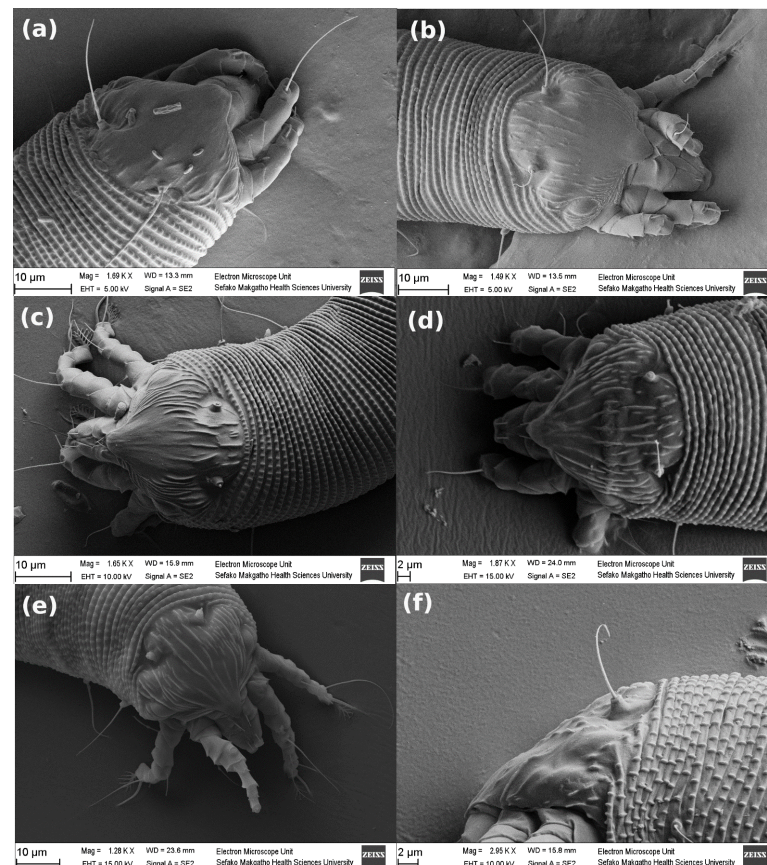


Figure 6. Prodorsal shield ornamentation in *Colomerus* specimens, showing gradation from smooth

to ridged. Note the eye-like pattern on the lateral surface of adult specimens. (a) Smooth with only a few ridges on the lateral edges. (b) Nearly smooth, with a few weak ridges between setae *sc*. (c) Smooth anteriorly with strong ridges between *sc*. (d) Strong ridges with broken median and admedian lines. (e) Strong ridges with complete median and admedian lines. (f) Immature specimen showing pebbled appearance and no visible eye-like pattern.

3.2.3. Coxal Area and Genitalia

The coxal area could be observed on 31 females (21 from erinea and 10 from buds), two males (one each from erinea and buds), and three immature (all from erinea) specimens (Figure 7). Consistent with the diagnosis of the *Colomerus* genus, the female genital coverflap displayed two uneven rows of ridges, while the male genital region had one row of ridges. The number of ridges on the female genital coverflap could be counted in 23 specimens, where the anterior row typically had one or two more ridges, varying between 11 and 15, while the bottom row had 10 to 14 ridges. This did not differ between specimens collected from buds or erinea.

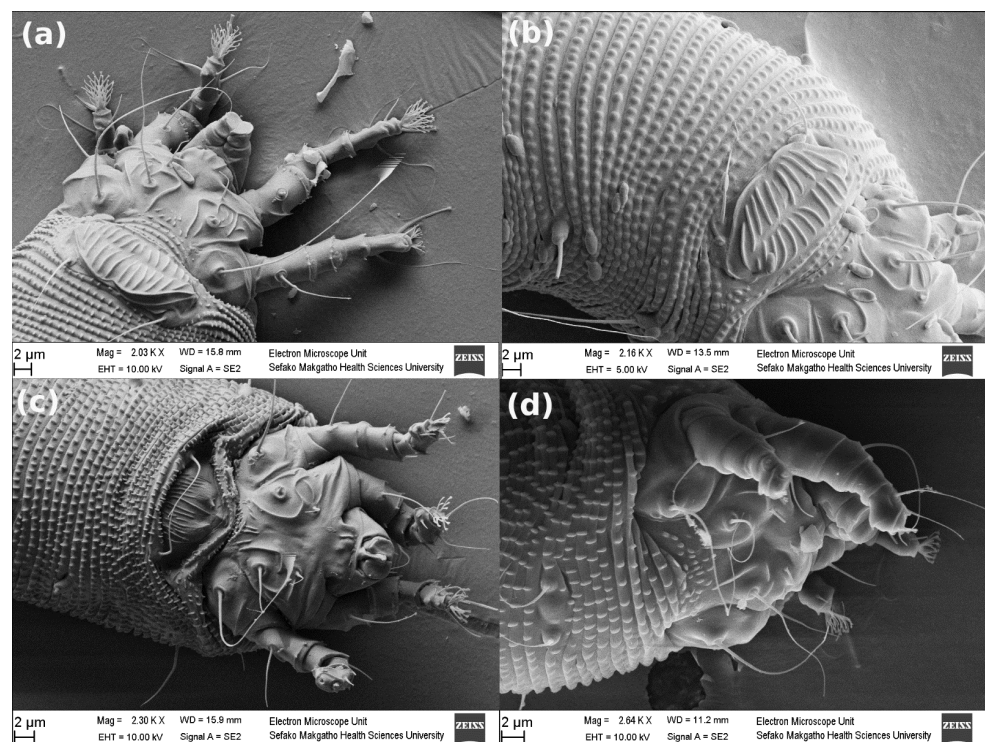


Figure 7. Coxal area and genitalia of *Colomerus* specimens. (a,b) Females. (c) Male. (d) Immature.

3.2.4. Legs

Legs (Figure 8) were of the typical eriophyoid shape, with all segments and leg setae present. An additional undescribed characteristic was observed, as some specimens had pointed spikes or protrusions along the distal ventral margin of the genu and/or tibia on one or both legs. Although the legs could be observed in all specimens, they were either not always orientated correctly, or the image was not clear enough to determine if these protrusions were present on all legs. In specimens in which the presence or absence of these protrusions could be determined with certainty, protrusions were observed more commonly on leg I (48% of erinea and 50% of bud specimens observed) than on leg II (32% of erinea and 27% of bud specimens observed). Both males examined had protrusions on their legs. There was no significant difference in the presence of these protrusions between mites collected from buds and erinea ($\chi^2 = 0.18$, $df = 1$, $p = 0.67$).

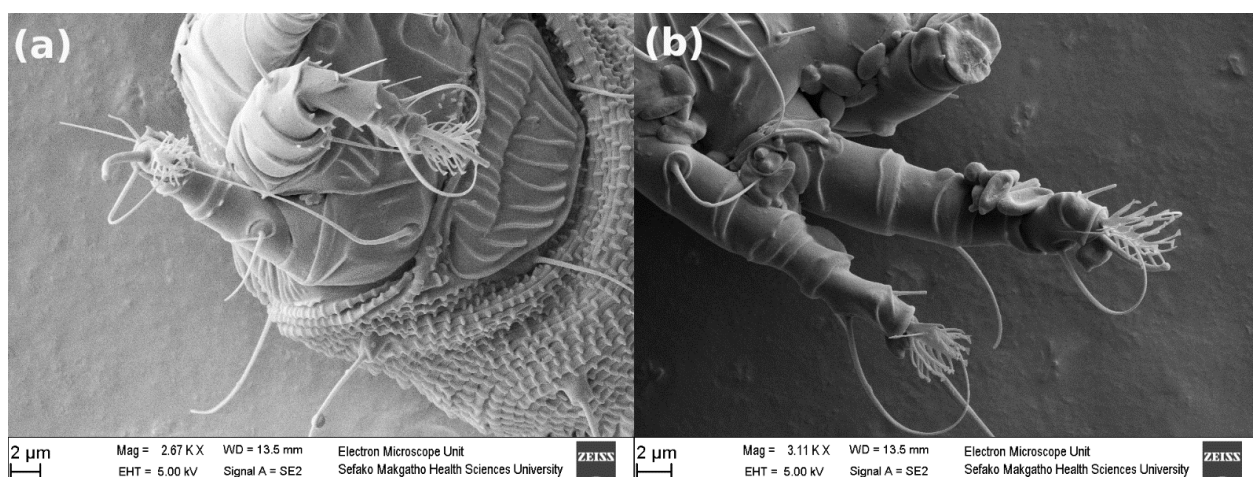


Figure 8. Leg ornamentation observed in *Colomerus* specimens. Note that these are both female specimens. (a) Pointed spikes or protrusions on the distal ventral margin of the genu and tibia. (b) Smooth distal ventral margin of the genu and tibia.

3.2.5. Empodia

The empodial (Figure 9) rays on the legs could be observed and counted on leg I in 24 specimens (20 from erinea and four from buds) and on leg II in 28 specimens (25 from erinea and three from buds). This count included two immature specimens with four-rayed empodia. In specimens in which both empodia I and II could be observed, there was no difference in the number of empodial rays ($n = 15$). Therefore, we assume that the number of empodial rays counted on any empodium was representative of all empodia of that specimen and report the results accordingly (Table S2). Empodia of adult mites observed from erinea showed both five- and six-rayed individuals of which 70% were five-rayed, while all mites observed from buds had six-rayed empodia. The association of six-rayed individuals with buds and five-rayed individuals with erinea was significant ($\chi^2 = 106.9$, $df = 1$, $p = 4.6 \times 10^{-25}$). In some specimens, rays were relatively simple and easy to count, whereas in others the empodium shape was more complex.

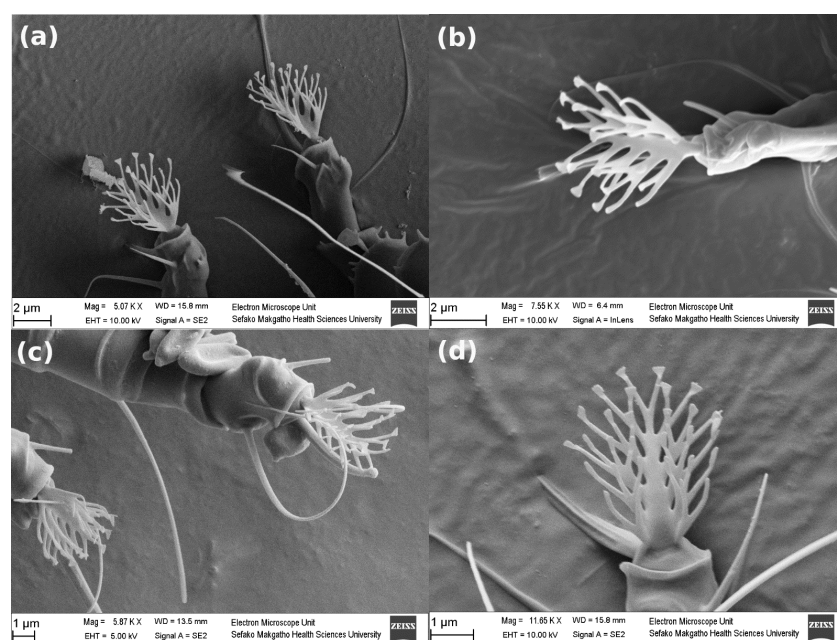


Figure 9. Empodial rays observed in *Colomerus* specimens. (a) Five-rayed empodia in a specimen

from erinea. (b) Five-rayed empodium in a specimen from erinea. (c) Six-rayed empodia in a specimen from buds. (d) Six-rayed empodium in a specimen from erinea.

3.2.6. Microtubercles

The surface microtubercles could clearly be observed in all specimens (Figures 10 and 11). Dorsal and ventral microtubercle shape did not differ greatly, with the dorsal microtubercles slightly larger and easier to discern. The shape varied from rounded, through oval to sharply pointed. Pointed microtubercles were easy to distinguish, as they displayed a sharp spike that projected over the posterior edge of the annuli. However, round and oval microtubercles were harder to distinguish, as a gradation of shape could be observed. Overall, 84% of mites from erinea and 77% of mites from buds had rounded or oval microtubercles, with no significant difference between the plant niches ($\chi^2 = 2.1$, $df = 2$, $p = 0.36$). Microtubercles observed dorsally extended to between the 12th and eighth annuli from the posterior end, after which 6–8 annuli were bare, followed by 2–4 annuli with small sharp spikes. Ventral microtubercles were present on all annuli, but faded and covered a smaller area posteriorly, followed by sharp spikes on the last few annuli from setae *f*. This arrangement did not vary on individuals with different microtubercle shapes.

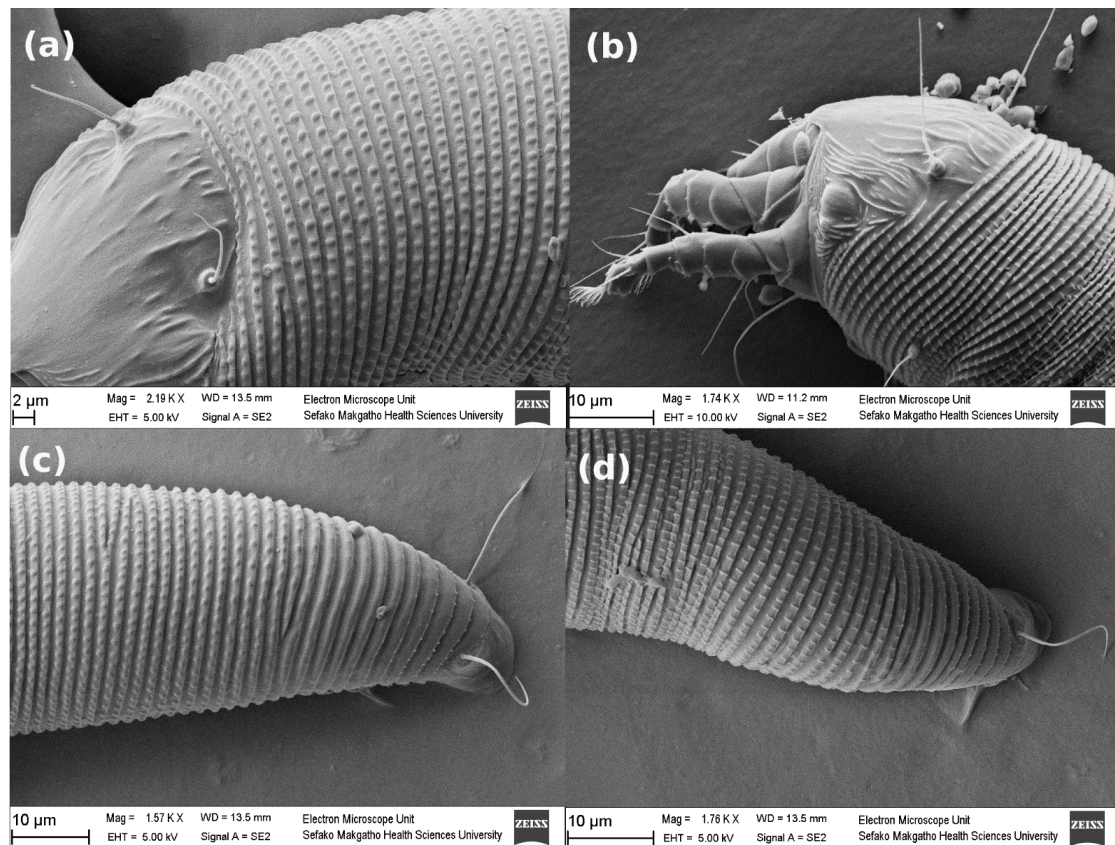


Figure 10. Dorsal microtubercles observed in *Colomerus* specimens. (a,c) Rounded microtubercles on the anterior and posterior opisthosoma, respectively. (b,d) Sharply pointed microtubercles on the anterior and posterior opisthosoma, respectively.

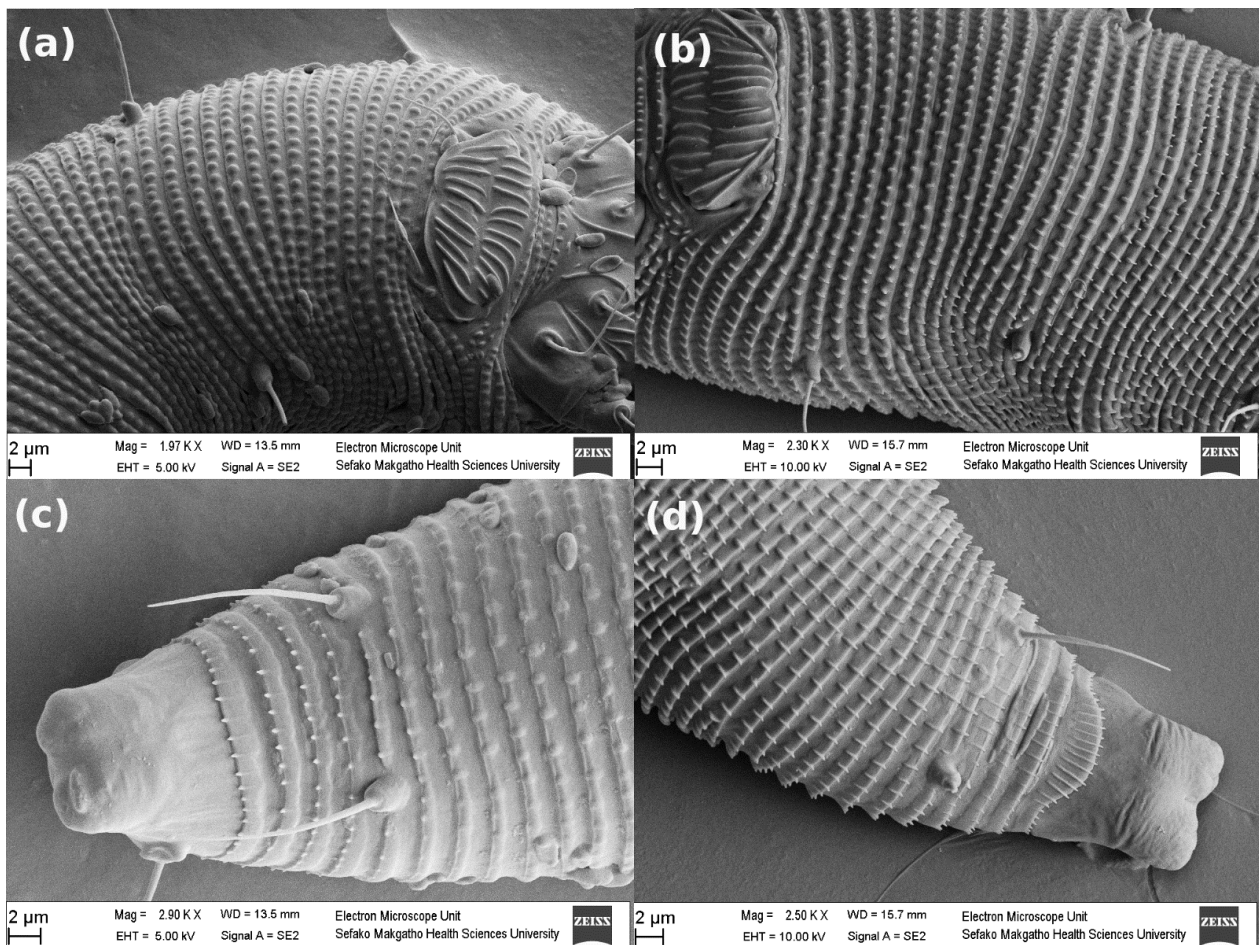


Figure 11. Ventral microtubercles observed in *Colomerus* specimens. (a,c) Rounded microtubercles on the anterior and posterior opisthosoma, respectively. (b,d) Sharply pointed microtubercles on the anterior and posterior opisthosoma, respectively.

3.2.7. Associations of Characteristics

No two characteristics were exclusively associated, but certain characteristic combinations were found more commonly than others. In specimens where two characteristics could be observed, a strongly patterned prodorsal shield was significantly, but not exclusively, associated with five-rayed empodia ($n = 18$, $\chi^2 = 100.0$, $df = 3$, $p = 1.6 \times 10^{-21}$) and rounded microtubercles ($n = 30$, $\chi^2 = 52.0$, $df = 3$, $p = 3.0 \times 10^{-11}$). Other characteristic states did not show significant associations. This variation of characteristic states in both plant niches is consistent with the genetic results from the same site, where all genetic groups were present in both buds and erinea (Figure 12).

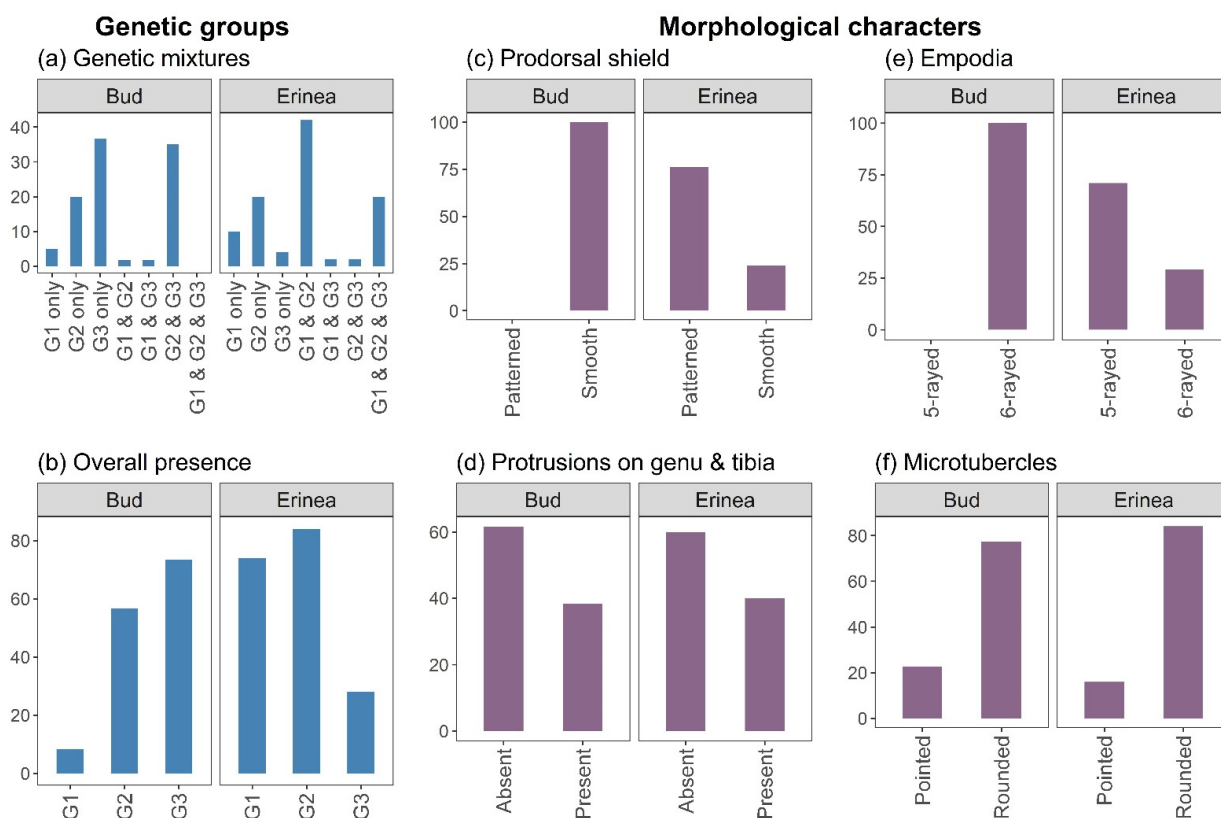


Figure 12. Comparison of genetic (a,b) and morphological (c–f) analyses at a single site (site 7, Table S1). For ease of comparison, all *y*-axes are plotted as percentages of samples tested (a,b) or individuals observed (c–f).

4. Discussion

The taxonomic status and diversity of *C. vitis* as a complex of multiple species or a single species consisting of multiple strains has been debated for decades [2–4]. Craemer and Saccaggi [4] detailed this confusion and emphasised the need for proper and detailed description of eriophyoid mites and a revision of grapevine *Colomerus* species, particularly that of the mites currently recognised as *C. vitis*. In this study, integration of advanced molecular and morphological tools revealed five diverged genetic clusters that likely represent separate species with no clear morphological differentiation.

4.1. Grapevine Eriophyoid Mites Likely Include Five Distinct Species

The analyses of COI sequences showed the presence of five well-supported phylogenetic clusters with low intragroup divergence and high intergroup divergence, estimated as *p*-distances. In assessments of conspecificity based on genetic distances, groups of phylogenetically similar sequences with intragroup *p*-distances less than 2–3% are considered to belong to the same species [42–44]. The intragroup max *p*-distance of each phylogenetic group reported in this study did not exceed 1.57%, which falls below the generally accepted threshold for species delimitation. Furthermore, the nonoverlap between intra- and intergroup *p*-distances supports the hypothesis that each of the five clusters represents a distinct species. However, previous studies in eriophyoid mites have reported intraspecific *p*-distances between 0% and 13%, and interspecific *p*-distances between 7% and 26% [16,23,25,45]. These ranges are much wider than those usually found among conspecific sequences in barcoding studies [44,46], implying either that eriophyoid species have atypically high intraspecific genetic diversity, or that many currently recognised species are in fact complexes of morphologically cryptic species.

4.2. Phylogeography of Grapevine *Colomerus* Mites

Three of the five groups identified in this study comprised sequences from a single country. Although the data available for analyses were limited, they suggested that some of the genetic groups may be geographically separated, while others may be cosmopolitan. This type of phylogeographic pattern has been observed in other eriophyoid species complexes, where a single lineage is widespread while others are localised [47]. Understanding whether this is indeed the case for grapevine *Colomerus* will require analyses of a much larger and geographically diverse dataset than that included in the present study. An interesting possibility is that different genetic groups are more frequently found in some world regions, which could be the case for G4 in the USA and G5 in Iran, because they evolved on the different wild *Vitis* species present in those regions. At this point, our small dataset only allows for speculation, and this hypothesis would have to be investigated by screening wild and cultivated *Vitis* worldwide.

4.3. LT-SEM Enhances Observable Morphological Detail

SEM images in the current study showed detailed variation in features of *Colomerus* specimens collected from grapevine buds and erinea. Cryo-SEM made it possible to observe such features without the shrinking artefacts commonly seen following conventional SEM preparation. All characteristics showed variation consistent with the published literature and were found in mites from both buds and erinea. Only two characteristics were consistently, but not exclusively, found in mites collected from buds: a smooth prodorsal shield and six-rayed empodia (Table S2). Selected features are discussed in more detail below.

4.3.1. Prodorsal Shield

The variability in prodorsal shield ornamentation is consistent with different *C. vitis* descriptions [3,5,8,48,49], but the observation of a smooth prodorsal shield in all dorsally-viewed specimens from buds and 15% from erinea was unexpected. With traditional slide-mounting techniques, there is a risk of over-clearing the specimen, resulting in less visible prodorsal shield ornamentation. It may be that, in the past, when specimens with reduced prodorsal shield ornamentation were observed, it was assumed that this was due to over-clearing and, thus, was not considered diagnostic. However, cryo-SEM precludes over-clearing of the mite; thus, this method can confirm that a large percentage of grapevine *Colomerus* specimens do, in fact, have smooth prodorsal shields.

It must be noted that the smooth prodorsal shield might indicate the presence of deutogynes, as they typically have reduced ornamentation compared to protogynes [50]. A deutogyne of *C. vitis* was described by Bagdasarian [8], but his depiction of it was not clear enough for comparison. However, considering that these samples were taken in March (late summer, and still very hot at the sampling site), if deutogynes were present in the population, one would expect to see a mixture of both protogynes and deutogynes in the samples. Thus, it is unlikely that these types represent a deutogyne form.

4.3.2. Coxal Area and Genitalia

Totals of 11–14 and 9–14 ridges were observed in the top and bottom row, respectively, of the genital coverflap of female specimens observed. This is less than reported by Keifer [3] for *C. vitis* (more than 16), but consistent with other descriptions of both *C. vitis* and *C. oculivitis* [4,6,7]. To avoid confusion, it should be noted that in Halawa et al.'s [6] revision of *Colomerus* in Egypt, they reported a third type of female genital coverflap: one with a single row of 16 ridges. This is incorrect, and the specimens depicted for that "type" are in fact male (See Figures 12 and 13 in Halawa et al. [6]).

4.3.3. Legs and Empodia

Attiah [7] noted that *C. oculivitis* had shorter legs than *C. vitis*. We did not measure leg length in the SEM images, as such measures could easily be inaccurate and, thus, misleading

due to three-dimensional orientation. However, we did not note visible variation in leg length other than that associated with immature specimens. In contrast, empodia clearly varied, with five- and six-rayed forms observed, as well as variation in complexity. The complex empodia did not prohibit counting the number of rays in the SEM images, but it may present challenges in the analysis of slide-mounted specimens. Where possible, fore- and hindleg empodia on both sides of a specimen were observed, and we did not find variation in empodial rays or shape within a specimen. Empodia observed on mites from buds all had six-rayed empodia, which appears to lend credence to the hypothesis of Craemer and Saccaggi [4] that *C. oculivitis* may represent the bud form of the mite. However, the empodia could only be observed on four specimens from buds, and six-rayed empodia were also observed in specimens from erinea. Thus, this finding should be viewed with care and interpreted in conjunction with other characteristics and the genetic results.

4.3.4. Microtubercles

Craemer and Saccaggi [4] noted variation in the shape of the microtubercles and recommended the inclusion of this characteristic in studying the grapevine *Colomerus* species; however, Halawa et al. [6] subsequently showed that, although variation was present, the shape of the microtubercles could not be used to distinguish between types of *C. vitis*. Our findings agree with the latter study, in that microtubercle shape was not associated with specimens from either buds or erinea and could not be linked to any other characteristic in our specimens.

5. Conclusions

We propose that the grapevine mite known as *C. vitis* is in fact a complex of at least five species that are genetically distinct and morphologically variable. The morphological variation, however, is not distinct to specific genetic groups, and the species cannot at this time be separated on the basis of morphology. We propose that *C. vitis* instead be referred to as a species complex, or as “*C. vitis sensu lato*”, as is the practice for very similar or identical species within a complex.

Our results additionally raise many questions which would not have been evident before, and we encourage further study in these areas. In particular, an integrative approach using genetic (sequencing and phylogenetic reconstruction), morphological (traditional slide-mounting and SEM), and biological (plant symptomology) analyses on the same sample from the same plant from the same niche would yield substantial insights into the associations of genetic, morphological, and biological diversity of these mites. Furthermore, wider sampling and analysis of genetic sequences from *Colomerus* mites from wild and cultivated grapevines around the world will increase the resolution and reveal the extent of genetic variation globally.

Supplementary Materials: The following supporting information can be downloaded at <https://www.mdpi.com/article/10.3390/d14050342/s1>: Table S1. Sampling sites and collection details of *Colomerus* mites collected from grapevine vineyards and fresh grapes for this study. The nearest town to the collection site is recorded for South African collections. The number of samples and which analyses they were used for are included. For use in multiplex PCR and DNA sequencing, a “sample” consists of collection of pooled mites collected from a single plant niche. For SEM imaging, a “sample” consists of a single mite.; Table S2. Summary of morphological characters observed using cryo-SEM on individual *Colomerus* specimens collected directed from buds and erinea. Only characters which showed variation between specimens are noted for comparison here.

Author Contributions: Conceptualisation, D.L.S., E.A., and B.v.A.; methodology, D.L.S., C.P., N.P.N.-N., and B.v.A.; formal analysis, D.L.S., P.M., and N.P.N.-N.; investigation, P.M., C.P., N.P.N.-N., and J.W.-S.; resources, E.A., J.W.-S., and B.v.A.; data curation, D.L.S. and P.M.; writing—original draft preparation, D.L.S. and B.v.A.; writing—review and editing, D.L.S., P.M., C.P., N.P.N.-N., E.A., J.W.-S., and B.v.A.; visualisation, D.L.S. and B.v.A.; supervision, B.v.A.; project administration, B.v.A.; funding acquisition, B.v.A. All authors have read and agreed to the published version of the manuscript.

Funding: This research was funded by Winetech (Wine Industry Network of Expertise and Technology), South Africa (Grant GenUS BvA 18-01). PM received partial bursaries from Winetech and Stellenbosch University.

Institutional Review Board Statement: Not applicable.

Informed Consent Statement: Not applicable.

Data Availability Statement: The sequences generated in this study were deposited on GenBank under the accession numbers ON060625-ON060655.

Acknowledgments: We express sincere thanks for Charnie Craemer, who recognised and initiated work in this taxon. Much of the work presented in this article stems from her initial research and insight into *Colomerus*, without which this study would not have been possible. P.M. received support from Winetech and Stellenbosch University.

Conflicts of Interest: The authors declare no conflict of interest.

References

1. Duso, C.; De Lillo, E. 3.2.5 Grape. In *World Crop Pests*; Elsevier: Amsterdam, The Netherlands, 1996; Volume 6, pp. 571–582. ISBN 9780444886286.
2. Smith, L.M.; Stafford, E.M. The Bud Mite and the Erineum Mite of Grapes. *Hilgardia* **1948**, *18*, 317–334. [[CrossRef](#)]
3. Keifer, H.H. Eriophyid Studies XIV. *Bull. Calif. Dep. Agric.* **1944**, *33*, 1–24.
4. Craemer, C.; Saccaggi, D.L. Frequent Quarantine Interception in South Africa of Grapevine *Colomerus* Species (Trombidiformes: Prostigmata: Eriophyidae): Taxonomic and Distributional Ambiguities. *Int. J. Acarol.* **2013**, *39*, 239–243. [[CrossRef](#)]
5. Smith Meyer, M.; Ueckermann, E.A. African Eriophyoidea: The Genus *Colomerus* Newkirk & Keifer, 1971 (Acari: Eriophyidae). *Phytophylactica* **1990**, *22*, 15–21.
6. Halawa, A.M.; Ebrahim, A.A.; Abdullah, A.A.M.; Mohamed, A.A. Taxonomical Revision of the Genus *Colomerus* Newkirk & Keifer (Acari: Eriophyidae) in Egypt. *Middle East J. Agric. Res.* **2015**, *4*, 67–76.
7. Attiah, H.H. *Eriophyes oculivitis* n. Sp., a New Bud Mite Infesting Grapes in the U.A.R. *Bull. Soc. Entomol. Egypt* **1967**, *51*, 17–19.
8. Bagdasarian, A.T.T. *The Eriophyoid Mites of Fruit Trees and Shrubs of Armenia*; Akademii Nauk Armyanskoi SSR [Academy of Science, Armenian SSR]: Yerevan, Armenia, 1981.
9. Carew, M.E.; Goodisman, M.A.D.; Hoffmann, A.A. Species Status and Population Genetic Structure of Grapevine Eriophyoid Mites. *Entomol. Exp. Appl.* **2004**, *111*, 87–96. [[CrossRef](#)]
10. Valenzano, D.; Tumminello, M.T.; Gualandri, V.; de Lillo, E.; Teresa, M.; Valeria, T.; de Lillo, E. Morphological and Molecular Characterization of the *Colomerus vitis* Erineum Strain (Trombidiformes: Eriophyidae) from Grapevine Erinea and Buds. *Exp. Appl. Acarol.* **2020**, *80*, 183–201. [[CrossRef](#)]
11. Bickford, D.; Lohman, D.J.; Sodhi, N.S.; Ng, P.K.L.; Meier, R.; Winker, K.; Ingram, K.K.; Das, I. Cryptic Species as a Window on Diversity and Conservation. *Trends Ecol. Evol.* **2007**, *22*, 148–155. [[CrossRef](#)] [[PubMed](#)]
12. Skoracka, A.; Magalhães, S.; Rector, B.G.; Kuczyński, L. Cryptic Speciation in the Acari: A Function of Species Lifestyles or Our Ability to Separate Species? *Exp. Appl. Acarol.* **2015**, *67*, 165–182. [[CrossRef](#)] [[PubMed](#)]
13. Skoracka, A. Host Specificity of Eriophyoid Mites: Specialists or Generalists? *Biol. Lett.* **2006**, *43*, 289–298.
14. Petanović, R. Towards an Integrative Approach to Taxonomy of Eriophyoidea (Acari, Prostigmata)—An Overview. *Ecol. Montenegrina* **2016**, *7*, 580–599. [[CrossRef](#)]
15. Navajas, M.; Navia, D. DNA-Based Methods for Eriophyoid Mite Studies: Review, Critical Aspects, Prospects and Challenges. *Exp. Appl. Acarol.* **2010**, *51*, 257–271. [[CrossRef](#)]
16. Skoracka, A.; Dabert, M. The Cereal Rust Mite *Abacarus hystrix* (Acari: Eriophyoidea) Is a Complex of Species: Evidence from Mitochondrial and Nuclear DNA Sequences. *Bull. Entomol. Res.* **2010**, *100*, 263–272. [[CrossRef](#)]
17. Skoracka, A.; Kuczyski, L.; Santos De Mendonça, R.; Dabert, M.; Szydło, W.; Knihinicki, D.; Truol, G.; Navia, D. Cryptic Species within the Wheat Curl Mite *Aceria tosichella* (Keifer) (Acari: Eriophyoidea), Revealed by Mitochondrial, Nuclear and Morphometric Data. *Invertebr. Syst.* **2012**, *26*, 417–433. [[CrossRef](#)]
18. Miller, A.D.; Skoracka, A.; Navia, D.; de Mendonça, R.S.; Szydło, W.; Schultz, M.B.; Michael Smith, C.; Truol, G.; Hoffmann, A.A. Phylogenetic Analyses Reveal Extensive Cryptic Speciation and Host Specialization in an Economically Important Mite Taxon. *Mol. Phylogenet. Evol.* **2013**, *66*, 928–940. [[CrossRef](#)] [[PubMed](#)]
19. Li, H.-S.; Xue, X.-F.; Hong, X.-Y. Cryptic Diversity in Host-Associated Populations of *Tetra pinnatifidae* (Acari: Eriophyoidea): What Do Morphometric, Mitochondrial and Nuclear Data Reveal and Conceal? *Bull. Entomol. Res.* **2014**, *104*, 221–232. [[CrossRef](#)] [[PubMed](#)]
20. Skoracka, A.; Lewandowski, M.; Rector, B.G.; Szydło, W.; Kuczy, L. Spatial and Host-Related Variation in Prevalence and Population Density of Wheat Curl Mite (*Aceria tosichella*) Cryptic Genotypes in Agricultural Landscapes. *PLoS ONE* **2017**, *12*, e0169874. [[CrossRef](#)]

21. Laska, A.; Majer, A.; Szydło, W.; Karpicka-Ignatowska, K.; Hornyák, M.; Labrzycka, A.; Skoracka, A. Cryptic Diversity within Grass-Associated *Abacarus* Species Complex (Acariformes: Eriophyidae), with the Description of a New Species, *Abacarus plumiger* n. sp. *Exp. Appl. Acarol.* **2018**, *76*, 1–28. [[CrossRef](#)] [[PubMed](#)]
22. Cvrković, T.; Chetverikov, P.; Vidović, B.; Petanović, R. Cryptic Speciation within *Phytoptus avellanae* s.l. (Eriophyoidea: Phytoptidae) Revealed by Molecular Data and Observations on Molting *Tegonotus*-like Nymphs. *Exp. Appl. Acarol.* **2016**, *68*, 83–96. [[CrossRef](#)] [[PubMed](#)]
23. Lewandowski, M.; Skoracka, A.; Szydło, W.; Kozak, M.; Druciarek, T.; Griffiths, D.A. Genetic and Morphological Diversity of *Trisetacus* Species (Eriophyoidea: Phytoptidae) Associated with Coniferous Trees in Poland: Phylogeny, Barcoding, Host and Habitat Specialization. *Exp. Appl. Acarol.* **2014**, *63*, 497–520. [[CrossRef](#)] [[PubMed](#)]
24. Chetverikov, P.E.; Cvrković, T.; Efimov, P.G.; Klimov, P.B.; Petanović, R.U.; Romanovich, A.E.; Schubert, M.A.; Sukhareva, S.I.; Zukoff, S.N.; Amrine, J. Molecular Phylogenetic Analyses Reveal a Deep Dichotomy in the Conifer-Inhabiting Genus *Trisetacus* (Eriophyoidea: Nalepellidae), with the Two Lineages Differing in Their Female Genital Morphology and Host Associations. *Exp. Appl. Acarol.* **2020**, *81*, 287–316. [[CrossRef](#)] [[PubMed](#)]
25. Živković, Z.; Vidović, B.; Jojić, V.; Cvrković, T.; Petanović, R. Phenetic and Phylogenetic Relationships among *Aceria* spp. (Acari: Eriophyoidea) Inhabiting Species within the Family Brassicaceae in Serbia. *Exp. Appl. Acarol.* **2017**, *71*, 329–343. [[CrossRef](#)]
26. Saccaggi, D.L.; Arendse, M.; Wilson, J.R.U.; Terblanche, J.S. Contaminant Organisms Recorded on Plant Product Imports to South Africa 1994–2019. *Sci. Data* **2021**, *8*, 83. [[CrossRef](#)] [[PubMed](#)]
27. Folmer, O.; Black, M.; Hoeh, W.; Lutz, R.; Vrijenhoek, R. DNA Primers for Amplification of Mitochondrial Cytochrome c Oxidase Subunit I from Diverse Metazoan Invertebrates. *Mol. Mar. Biol. Biotechnol.* **1994**, *3*, 294–299. [[CrossRef](#)]
28. Kearse, M.; Moir, R.; Wilson, A.; Stones-Havas, S.; Cheung, M.; Sturrock, S.; Buxton, S.; Cooper, A.; Markowitz, S.; Duran, C.; et al. Geneious Basic: An Integrated and Extendable Desktop Software Platform for the Organization and Analysis of Sequence Data. *Bioinformatics* **2012**, *28*, 1647–1649. [[CrossRef](#)]
29. Biomatters. User Manual Geneious Prime. *Data Base* **2012**, *3304*, 1–322.
30. Katoh, K.; Standley, D.M. MAFFT Multiple Sequence Alignment Software Version 7: Improvements in Performance and Usability. *Mol. Biol. Evol.* **2013**, *30*, 772–780. [[CrossRef](#)] [[PubMed](#)]
31. Minh, B.Q.; Schmidt, H.A.; Chernomor, O.; Schrempf, D.; Woodhams, M.D.; Von Haeseler, A.; Lanfear, R.; Teeling, E. IQ-TREE 2: New Models and Efficient Methods for Phylogenetic Inference in the Genomic Era. *Mol. Biol. Evol.* **2020**, *37*, 1530–1534. [[CrossRef](#)] [[PubMed](#)]
32. Lanfear, R.; Calcott, B.; Ho, S.Y.W.; Guindon, S. PartitionFinder: Combined Selection of Partitioning Schemes and Substitution Models for Phylogenetic Analyses. *Mol. Biol. Evol.* **2012**, *29*, 1695–1701. [[CrossRef](#)]
33. Chernomor, O.; Von Haeseler, A.; Minh, B.Q. Terrace Aware Data Structure for Phylogenomic Inference from Supermatrices. *Syst. Biol.* **2016**, *65*, 997–1008. [[CrossRef](#)] [[PubMed](#)]
34. Kalyaanamoorthy, S.; Minh, B.Q.; Wong, T.K.F.; Von Haeseler, A.; Jermini, L.S. ModelFinder: Fast Model Selection for Accurate Phylogenetic Estimates. *Nat. Methods* **2017**, *14*, 587–589. [[CrossRef](#)] [[PubMed](#)]
35. Guindon, S.; Dufayard, J.-F.; Lefort, V.; Anisimov, M.; Hordijk, W.; Gascuel, O. New Algorithms and Methods to Estimate Maximum-Likelihood Phylogenies: Assessing the Performance of PhyML 3.0. *Syst. Biol.* **2010**, *59*, 307–321. [[CrossRef](#)]
36. Hoang, D.T.; Chernomor, O.; Von Haeseler, A.; Minh, B.Q.; Vinh, L.S. UFBoot2: Improving the Ultrafast Bootstrap Approximation. *Mol. Biol. Evol.* **2017**, *35*, 518–522. [[CrossRef](#)]
37. Kumar, S.; Stecher, G.; Li, M.; Nkayaz, C.; Tamura, K. MEGA X: Molecular Evolutionary Genetics Analysis across Computing Platforms. *Mol. Biol. Evol.* **2018**, *35*, 1547–1549. [[CrossRef](#)] [[PubMed](#)]
38. Kimura, M. A Simple Method for Estimating Evolutionary Rates of Base Substitutions through Comparative Studies of Nucleotide Sequences. *J. Mol. Evol.* **1980**, *16*, 111–120. [[CrossRef](#)] [[PubMed](#)]
39. Rahbani, J.; Behzad, A.R.; Khashab, N.M.; Al-Ghoul, M. Characterization of Internal Structure of Hydrated Agar and Gelatin Matrices by Cryo-SEM. *Electrophoresis* **2013**, *34*, 405–408. [[CrossRef](#)] [[PubMed](#)]
40. Amrine, J.W.J.; Manson, D.C.M. Preparation, Mounting and Descriptive Study of Eriophyoid Mites. In *Eriophyoid Mites: Their Biology, Natural Enemies and Control*; Lindquist, E.E., Sabelis, M.W., Bruin, J., Eds.; Elsevier: Amsterdam, The Netherlands, 1996; pp. 383–396.
41. de Lillo, E.; Craemer, C.; Amrine, J.W., Jr.; Nuzzaci, G. Recommended Procedures and Techniques for Morphological Studies of Eriophyoidea (Acari: Prostigmata). *Exp. Appl. Acarol.* **2010**, *51*, 283–307. [[CrossRef](#)]
42. Meier, R.; Zhang, G.; Ali, F. The Use of Mean Instead of Smallest Interspecific Distances Exaggerates the Size of the “Barcoding Gap” and Leads to Misidentification. *Syst. Biol.* **2008**, *57*, 809–813. [[CrossRef](#)]
43. Navia, D.; Mendonça, R.S.; Ferragut, F.; Miranda, L.C.; Trincado, R.C.; Michaux, J.; Navajas, M. Cryptic Diversity in *Brevipalpus* Mites (Tenuipalpidae). *Zool. Scr.* **2013**, *42*, 406–426. [[CrossRef](#)]
44. Hebert, P.D.N.; Penton, E.H.; Burns, J.M.; Janzen, D.H.; Hallwachs, W. Ten Species in One: DNA Barcoding Reveals Cryptic Species in the Neotropical Skipper Butterfly *Astrartes fulgurator*. *Proc. Natl. Acad. Sci. USA* **2004**, *101*, 14812–14817. [[CrossRef](#)] [[PubMed](#)]
45. Skoracka, A.; Kuczyński, L.; Szydło, W.; Rector, B. The Wheat Curl Mite *Aceria tosichella* (Acari: Eriophyoidea) Is a Complex of Cryptic Lineages with Divergent Host Ranges: Evidence from Molecular and Plant Bioassay Data. *Biol. J. Linn. Soc.* **2013**, *109*, 165–180. [[CrossRef](#)]

46. Meyer, C.P.; Paulay, G. DNA Barcoding: Error Rates Based on Comprehensive Sampling. *PLoS Biol.* **2005**, *3*, e422. [[CrossRef](#)]
47. Skoracka, A.A.; Rector, B.; Kuczyński, L.; Szydło, W.; Hein, G.; French, R. Global Spread of Wheat Curl Mite by Its Most Polyphagous and Pestiferous Lineages. *Ann. Appl. Biol.* **2014**, *165*, 222–235. [[CrossRef](#)]
48. Mathez, F. Contribution to the Study of the Morphology and Biology of *Eriophyes vitis* Pgst., the Causal Agent of Grapevine Erineum. *Mitt. Schweiz. Entomol. Ges.* **1965**, *37*, 233–283.
49. Manson, D.C.M. Eriophyinae (Arachnida: Acari: Eriophyoidea). *Fauna N. Z.* **1984**, *5*, 128. [[CrossRef](#)]
50. Manson, D.C.M.; Oldfield, G.N. Life forms, deutero-gyny, diapause and seasonal development. In *Eriophyoid Mites: Their Biology, Natural Enemies and Control*; Lindquist, E.E., Sabelis, M., Bruin, J., Eds.; Elsevier: Amsterdam, The Netherlands, 1996; pp. 173–183.